

Statistical Properties of Eigenstates in three-dimensional Mesoscopic Systems with Off-diagonal or Diagonal Disorder

Branislav K. Nikolic[†]

Department of Physics and Astronomy, SUNY at Stony Brook, Stony Brook, New York 11794-3800

The statistics of eigenfunction amplitudes are studied for mesoscopic disordered electronic systems of finite size. The exact eigenspectrum and eigenstates are obtained by solving numerically the nearest-neighbor tight-binding Hamiltonian defined on a three-dimensional lattice. Disorder is introduced either in the potential on-site energy (“diagonal”) or in the hopping (“off-diagonal”) between single s-orbitals residing on each site. The samples are characterized by the exact zero-temperature conductance computed using real-space Green function technique and related Landauer-type formula. The comparison of eigenstate statistics in two models of disorder shows sample-specific details which are not fully taken into account by the value of conductance, shape of the sample and dimensionality. The distribution functions are also contrasted with the universal predictions of Random Matrix Theory valid in the infinite conductance limit.

PACS numbers: 72.15.Rn, 73.23.-b, 05.40.-a

The disorder induced localization-delocalization (LD) transition in solids has been one of the most vigorously pursued problems in condensed matter physics since the seminal work of Anderson.¹ In thermodynamic limit, strong enough disorder generates a zero-temperature critical point in $d > 2$ dimensions,² as a result of quantum interference effects. Thus, research in the “pre-mesoscopic” era³ was mostly directed toward the viewpoint provided by the theory of critical phenomena.⁴ The advent of mesoscopic quantum physics⁵ has unearthed large fluctuations, induced by quantum coherence and randomness of disorder,⁶ of various physical quantities⁷ (e.g., conductance, local density of states, current relaxation times, etc.), even well into the delocalized phase. Thus, complete understanding of the LD transition requires to examine full distribution functions of relevant quantities.⁸ Especially interesting are deviations of their asymptotic tails, caused by the incipient localization, from the (usually) Gaussian distributions expected in the limit of infinite dimensionless conductance $g = G/G_Q$ (in units of the conductance quantum $G_Q = 2e^2/h$). This paper presents the study of such type—numerical computation of the statistics of eigenfunction amplitudes in a finite-size three-dimensional (3D) nanoscale (composed of ~ 1000 atoms) mesoscopic disordered conductors. The 3D conductors are often “neglected” in favor of the more popular (and tractable) playgrounds—two-dimensional systems (2D), where one can study states resembling 3D critical wave functions in a wide range of systems sizes and disorder strengths,⁹ or quasi one-dimensional systems¹⁰ where analytical techniques can handle even non-perturbative phenomena (like the ones at small g).^{11,12} In 3D systems critical eigenfunctions, exhibiting multifractal scaling, appear only at the mobility edge E_c which separates extended and localized states inside the energy band.

The essential physics of disordered conductors is captured by studying just the quantum dynamics of a non-interacting (quasi)particle in a random and confining

potential. This problem is classically non-integrable, thereby exhibiting quantum chaos. The concepts unifying disordered electron physics with the standard examples of quantum chaos¹³ come from the statistical approach to the properties of energy spectrum and corresponding eigenstates, which can not be computed analytically. While energy level statistics of disordered systems have been explored to a great extent,^{14,15} investigation of the statistics of eigenfunctions has been initiated only recently.¹⁶ These studies are not only divulging peculiar spectral properties of random Hamiltonians, but are relevant for the thorough understanding of various unusual features of quantum transport in diffusive metallic samples. The standard examples are long-time tails in the relaxation of current¹⁷ or log-normal tails (in $d = 2 + \epsilon$) of the distribution function of mesoscopic conductances.⁷ Also, tunneling experiments on quantum dots probe the coupling to external leads, which depends sensitively on the local properties of wave functions.¹⁸ Experiments which are the closest to directly delving into the microscopic structure of quantum chaotic or disordered wave functions exploit the correspondence between the Schrödinger and Maxwell equations in microwave cavities.¹⁹

The study of fluctuations and correlations of eigenfunction amplitudes^{16,20} in mesoscopic systems has led to the concept of the so-called pre-localized states.^{7,17,21} The notion refers to the states which have sharp amplitude peaks on the top of an extended background (in the 3D delocalized phase).²² These kind of states appear even in the diffusive, $\ell \ll L < \xi$, metallic ($g \gg 1$) regime, but are anomalously rare in such samples. Here ℓ is the elastic mean free path and ξ is the localization length (which plays the role of a phase transition correlation length⁶ ξ_c in $d \leq 2$). In order to get “experimental” feeling for the structure of states with unusually high amplitude spikes, an example is given on Fig. 1; this state is found in a special realization of quenched disorder (out of many randomly generated impurity config-

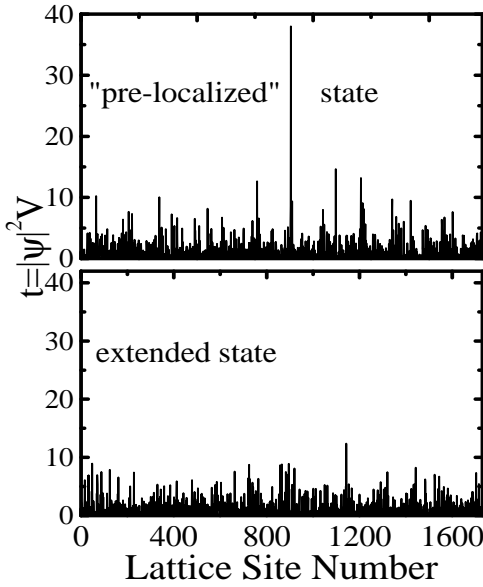


FIG. 1. An example of eigenstates in the band center of a delocalized phase. The average conductance at half filling is $g(E_F = 0) \approx 17$, entailing anomalous rarity of the “pre-localized” states. The disordered conductor is modeled by an Anderson model with diagonal disorder on a simple cubic lattice with 12^3 sites. For plotting of the eigenfunction values in 3D, the sites \mathbf{m} are mapped onto the lattice site numbers $\in \{1, \dots, 1728\}$ in a lexicographic order, i.e., $\mathbf{m} \equiv (m_x, m_y, m_z) \mapsto 144(m_x - 1) + 12(m_y - 1) + m_z$.

urations) inside the sample characterized by large average conductance. Thus, pre-localized states are putative precursors of LD transition and determine asymptotics of some of the distribution functions^{6,16} studied in open or closed mesoscopic systems. In $d \leq 2$, where all states are considered to be localized,⁴ pre-localized states have anomalously short localization radius¹⁶ when compared to “ordinary” localized states in low-dimensional systems. They underlie²¹ the multifractal scaling in weakly localized ($g \gg 1$) 2D conductors where $L < \xi = \xi_c$. In 3D the correlation length is always microscopic ($\sim \lambda_F$) in good metallic samples, and no multifractal scaling is expected.⁶ The appearance of small regions inside disordered solids where eigenstates can have large amplitudes seems to be a “strongly pronounced” analog^{9,19} of the phenomenon of scarring²³ (anomalous enhancement or suppression of quantum chaotic wave function intensity on the unstable periodic orbits in the corresponding classical system).

In general, the study of properties of wave functions on a scale smaller than ξ should probe quantum effects causing evolution of extended into localized states upon approaching the LD critical point. In the marginal two-dimensional case, the divergent (in the limit $L \rightarrow \infty$) weak localization (WL) correction²⁴ to the semiclassical Boltzmann conductivity provides an explanation of localization in terms of the interference between two ampli-

tudes to return to initial point along the same classical path in the opposite directions.²⁵ This simple quantum interference effect leads to a coherent backscattering (i.e., suppression of conductivity) in a time-reversal invariant systems without spin-orbit interaction. However, in 3D systems WL correction is not “strong” enough to provide a full microscopic picture of complicated quantum interference processes which are responsible for LD transition, and facilitate the expansion of “quantum intuition”.

Here I expose the results for the statistics of eigenfunction intensities $|\psi_\alpha(\mathbf{r})|^2$ in isolated 3D mesoscopic conductors characterized by two different types of microscopic disorder. Numerical methods employed make it possible to treat both perturbative and non-perturbative phenomena as well as the crossover realm in between. The statistical properties of eigenstates are embodied in the disorder-averaged distribution function^{9,21}

$$f(t) = \frac{1}{\rho(E)N} \left\langle \sum_{\mathbf{r}, \alpha} \delta(t - |\Psi_\alpha(\mathbf{r})|^2 V) \delta(E - E_\alpha) \right\rangle, \quad (1)$$

on N discrete points \mathbf{r} inside a sample of volume V . Here $\rho(E) = \sum_\alpha \delta(E - E_\alpha)$ is the mean level density at energy E . Averaging over disorder is denoted by $\langle \dots \rangle$. Normalization of eigenstates gives $\langle t \rangle = \int dt t f(t) = 1$. A finite-size disordered sample is modeled by a tight-binding Hamiltonian (TBH) with nearest neighbor hopping $t_{\mathbf{mn}}$

$$\hat{H} = \sum_{\mathbf{m}} \varepsilon_{\mathbf{m}} |\mathbf{m}\rangle \langle \mathbf{m}| + \sum_{\langle \mathbf{m}, \mathbf{n} \rangle} t_{\mathbf{mn}} |\mathbf{m}\rangle \langle \mathbf{n}|, \quad (2)$$

on a simple cubic lattice $16 \times 16 \times 16$. Each site \mathbf{m} contains a single orbital $\langle \mathbf{r} | \mathbf{m} \rangle = \psi(\mathbf{r} - \mathbf{m})$. Periodic boundary conditions are chosen in all directions. In a random hopping (RH) model the disorder is introduced by taking the off-diagonal matrix elements to be a uniformly distributed random variable, $1 - 2W_{\text{RH}} < t_{\mathbf{mn}} < 1$ (diagonal elements are zero, $\varepsilon_{\mathbf{m}} = 0$). The strength of the disorder is measured by W_{RH} . The other model studied here is a diagonally disordered (DD) Anderson model with potential energy $\varepsilon_{\mathbf{m}}$ on site \mathbf{m} drawn from the uniform distribution, $-W_{\text{DD}}/2 < \varepsilon_{\mathbf{m}} < W_{\text{DD}}/2$, with $t_{\mathbf{mn}} = 1$ being the unit of energy. The Hamiltonian (2) is a real symmetric matrix because time-reversal symmetry is assumed. The results for $f(t)$ in the samples described by the RH and DD Anderson models are shown on Figs. 2, 3 and Fig. 4, respectively. Although some of the samples are characterized by similar values of conductance, the eigenstates in the two models show different statistical behavior. In what follows the meaning of these findings is explained in the context of statistical approach to quantum systems with non-integrable classical dynamics. In particular, the results are compared to the universal predictions of Random Matrix Theory (RMT).

In the statistical approach¹⁵ of RMT the (random) Hamiltonian of a quantum chaotic system is replaced²⁶ by a random matrix drawn from an ensemble defined

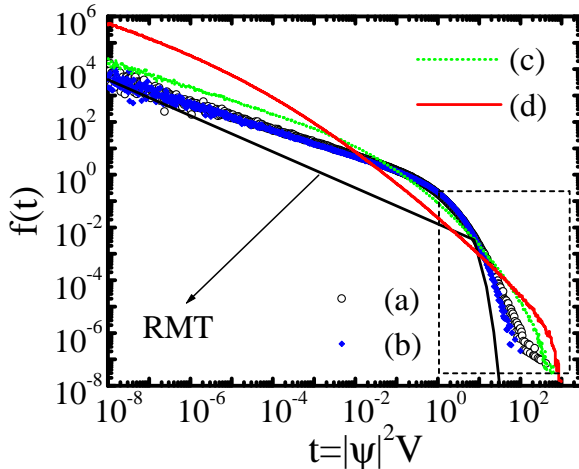


FIG. 2. Statistics of wave function intensities in the RH Anderson model, with $W_{\text{RH}} = 1$, on a simple cubic lattice with $N = 16^3$ sites. The distribution function $f(t)$, Eq. (1), is computed for the states around the following energies: (a) $E = 0$, (b) $E = 1.5$, (c) $E = 2.55$, and (d) $E = 2.75$. Disorder averaging is performed over $N_{\text{Ens}} = 40$ different samples. The Porter-Thomas distribution (3) is denoted by RMT. The part of the distributions inside the dashed box is enlarged on Fig. 3.

by the symmetries under time-reversal and spin-rotation. This leads to the Wigner-Dyson (WD) statistics for eigenvalues and Porter-Thomas (PT) distribution for eigenfunction intensities. For the Gaussian Orthogonal Ensemble (GOE), relevant for studies of time-reversal-invariant Hamiltonians like (2), the PT distribution is given by

$$f_{\text{PT}}^0(t) = \frac{1}{\sqrt{2\pi t}} \exp(-t/2). \quad (3)$$

The function $f_{\text{PT}}^0(t)$ is plotted as a reference on Figs. 2, 3 and Fig. 4. The predictions of RMT are universal, depending only on the symmetry properties of the relevant ensemble. They apply to the statistics of real disordered systems²⁸ in the limit $g \rightarrow \infty$ ($g = E_{\text{Th}}/\Delta$, where $\Delta = 1/\rho(E)$ is the mean energy level spacing and $E_{\text{Th}} = \hbar\mathcal{D}/L^2$ is the Thouless energy, set by the classical diffusion with diffusion constant \mathcal{D}). The spectral correlations in RMT are determined by logarithmic level repulsion which is independent of true dynamics.¹⁵ All sample-specific details are absorbed into the mean level spacing¹² Δ . Also, the level correlations are independent of the eigenstate correlations. The RMT answer (3) for the distribution function (1) was derived by Porter and Thomas²⁹ by assuming that the coordinate-representation eigenstate $\langle \mathbf{r} | \psi_\alpha \rangle$ in a disordered (or classically chaotic system) is a Gaussian random variable. The behavior of $\psi_\alpha(\mathbf{r})$, even within the framework of RMT, is simple only in the systems with unbroken or completely broken time-reversal symmetry (the only difference between the two limiting ensembles is the functional form

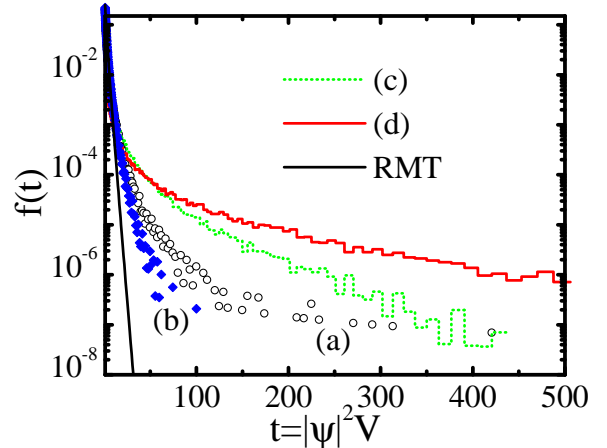


FIG. 3. Statistics of wave function intensities in the RH Anderson model, with $W_{\text{RH}} = 1$, on a simple cubic lattice with $N = 16^3$ sites. This Figure plots the same distributions $f(t)$ as the ones plotted on Fig. 2, in the range defined by the dashed square on Fig. 2. The same labels apply to both Figures.

of $f(t)$).³⁰ Thus, RMT implies statistical equivalence of eigenstates which equally test the random potential all over the sample; typical wave function has uniform amplitude, up to inevitable Gaussian fluctuations.

Microscopic theory brings corrections to the RMT results in the case of samples with finite g . In the finite-size systems level statistics follow RMT predictions in the ergodic regime, i.e., on the energy separation scale smaller than E_{Th} . Non-universal corrections to the spectral statistics³¹ or eigenfunction statistics³² (which describe the long-range correlations of wave functions) depend on dimensionality, shape of the sample, and conductance g . These deviations from RMT predictions grow with increasing disorder (i.e., lowering of g). At the LD transition wave functions acquire multifractal properties, while the critical level statistics become scale-independent.³³ For strong disorder or, at fixed disorder, for energies $|E|$ above the mobility edge $|E_c|$, wave functions are exponentially localized. A typical wave function decays as $\psi(r) = p(r) \exp(-r/\xi)$ from its maximum centered at an arbitrary point inside the sample of size $L > \xi$. Here $p(r)$ is a random function and approximately radial symmetry of decay is assumed. Since two states close in energy are localized at different points in space, there is almost no overlap between them. Therefore, the levels become uncorrelated and obey Poisson statistics. If $p(r) = c$ is simplified to a normalization constant, the distribution function of intensities is given by⁹

$$f_\xi(t) = \frac{\pi \xi^2}{2V} \frac{\ln(c^2 V/t)}{t}, \quad (4a)$$

$$c^2 = \frac{2}{\pi \xi^2} \left(1 - \left(1 + \frac{L}{\xi} \right) \exp(-L/\xi) \right)^{-1}, \quad (4b)$$

where a radially symmetric sample (radius $L/2$) is as-

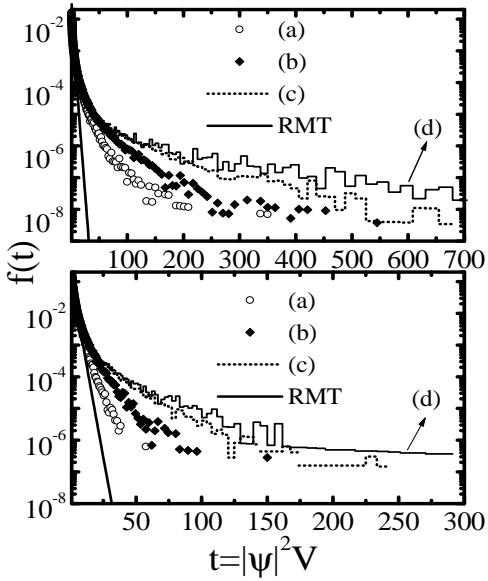


FIG. 4. Statistics of wave function intensities in the DD Anderson model on a simple cubic lattice with $N = 16^3$ sites. The distribution function $f(t)$, Eq. (1), is computed for the states around following energies. Upper panel, $W_{DD} = 10$: (a) $E = 0$, (b) $E = 6.0$, (c) $E = 7.45$, and (d) $E = 7.85$. Lower panel, $W_{DD} = 6$: (a) $E = 0$, (b) $E = 4.1$, (c) $E = 6.56$, and (d) $E = 6.7$. Disorder averaging is performed over $N_{Ens} = 40$ different samples. The Porter-Thomas distribution (3) is denoted by RMT.

sumed.

The distribution function $f(t)$ is equivalently given in term of its moments $b_q = \int dt t^q f(t)$. For GOE, the PT distribution (3) has moments $b_q^{\text{PT}} = 2^q V^{-q+1} \Gamma(q+1/2)/\Gamma(1/2)$. They are related to the moments $I_\alpha(q) = \int d\mathbf{r} |\Psi_\alpha(\mathbf{r})|^{2q}$ of the wave function intensity $|\Psi_\alpha(\mathbf{r})|^2$. In the finite g case the spatial correlations of wave function amplitudes at distances comparable to the system size are non-negligible. Therefore $I_\alpha(q)$ fluctuates from state to state and from sample to sample.¹⁶ In the universal regime $g \rightarrow \infty$ wave functions cover the whole volume with only short-range correlations (on the scale $|\mathbf{r}_1 - \mathbf{r}_2| \lesssim \ell$) persisting between $\Psi_\alpha(\mathbf{r}_1)$ and $\Psi_\alpha(\mathbf{r}_2)$. This means that integration in the definition of $I_\alpha(q)$ provides self-averaging and $I_\alpha(q)$ does not fluctuate in the universal limit, i.e., $I_\alpha(q) = b_q^{\text{PT}}$. Following Wegner,³⁴ individual states in the analysis to follow are characterized by an ensemble average of $I_\alpha(q)$

$$\bar{I}(q) = \Delta \left\langle \sum_{\mathbf{r}, \alpha} |\Psi_\alpha(\mathbf{r})|^{2q} \delta(E - E_\alpha) \right\rangle. \quad (5)$$

The moment $I_\alpha(2)$ is usually called inverse participation ratio (IPR). It is a one-number measure of the degree of localization (i.e., it measures the portion of space where the amplitude of the wave function differs markedly from zero). This becomes obvious from the scaling properties of moments $\bar{I}(q)$ with respect to the system size

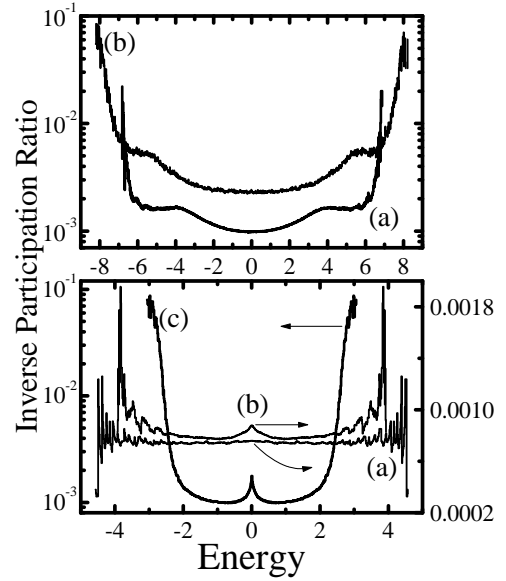


FIG. 5. Inverse Participation Ratio $\bar{I}(2)$, averaged over both 40 different conductors and small energy bins, of eigenstates in the RH and DD Anderson models on a simple cubic lattice with $N = 16^3$ sites. Top: diagonal disorder with (a) $W_{DD} = 6$, and (b) $W_{DD} = 10$. Bottom: off-diagonal disorder with (a) $W_{RH} = 0.25$, (b) $W_{RH} = 0.375$, and (c) $W_{RH} = 1$.

$$\bar{I}(q) \propto \begin{cases} L^{-d(q-1)} & \text{metal,} \\ L^0 & \text{insulator,} \\ L^{-d^*(q)(q-1)} & \text{critical.} \end{cases} \quad (6)$$

Here $d^*(q) < d$ is the fractal dimension. Its dependence on q is the hallmark of multifractality of wave functions. These functions are delocalized, but extremely inhomogeneous occupying only an infinitesimal fraction of the sample volume in thermodynamic limit. The IPR is affected by mesoscopic fluctuations which scale in metallic samples as²⁰ $\delta I_\alpha(2) \sim 1/g^2 \propto L^{4-2d}$. In the critical region ($g \sim 1$) fluctuations²⁰ are of the same order as the average value, which is then not enough to characterize the critical eigenstates (their IPR is not self-averaging³⁵ even though multifractal wave function extend through the whole sample).

I use $\bar{I}(2)$ (Fig. 5) as a rough guide in selecting eigenstates with different properties (especially in the delocalized phase). The second parameter used in the “selection procedure” is the conductance $g(E_F)$ (see below, Fig. 6) computed for a band filled up to the Fermi energy E_F equal to the state eigenenergy. The conductance as a function of band filling allows one to delineate delocalized from localized phase as well as to narrow down the critical region around LD transition point (which is defined by E_c when disorder strengths W_{RH} or W_{DD} are fixed). Upon inspection of these two parameters, a small window is placed around chosen energy, and $f(t)$ is computed for all eigenenergies whose eigenvalues fall inside the window. This provides a detailed information on the structure of eigenstates.

The average IPR for both RH and DD Anderson model is shown on Fig. 5. The models with random hopping³⁶ have attracted recently considerable attention inasmuch as they show a disorder induced quantum critical point in less than three dimensions,^{37,38} where delocalization occurs in the band center ($E = 0$). The real system which correspond to TBH (2) with off-diagonal disorder include doped semiconductors,³⁶ such as P-doped Si, where hopping matrix elements t_{mn} vary exponentially with the distances between the orbitals they connect, while diagonal on-site energies ε_m are nearly constant. The behavior of low-dimensional RH Anderson model goes against the standard mantra of the scaling theory of localization⁴ that all states in $d \leq 2$ are localized. This is actually known since the work of Dyson³⁹ on glasses. Also, the scaling theory for quantum wires with off-diagonal disorder requires two parameters⁴⁰ which depend on the microscopic model, thus breaking the celebrated universality in disordered electron problems. In 3D case explored here, the states in the band center are less extended than other delocalized states inside the band (Fig. 5). The off-diagonal disorder is not strong enough⁴¹ to localize all states in the band, in contrast to the usual case of diagonal disorder where whole band becomes localized⁴² for $W_{DD}^c > 16.5$.

The mobility edge for the strongest RH disorder $W_{RH} = 1$, as well as for DD models, is found by looking at an exact zero-temperature static conductance. This quantity (which is a Fermi surface property) is computed from the Landauer-type formula⁴³ (the factor of two here and in the density of states (8) is for spin degeneracy)

$$G(E_F) = \frac{2e^2}{h} \text{Tr}(\mathbf{t}(E_F)\mathbf{t}^\dagger(E_F)), \quad (7)$$

where transmission matrix $\mathbf{t}(E_F)$ is expressed in terms of the real-space (lattice) Green functions^{44,45} for the sample attached to two clean semi-infinite leads. To study the conductance in the whole band of the DD model, $t_{mn} = 1.5$ is used⁴⁵ for the hopping parameter in the leads. This mesoscopic computational technique “opens” the sample, thereby smearing the discrete levels of initially isolated system. Therefore, the spectrum of *sample+leads=infinite system* becomes continuous and conductance can be calculated at any E_F inside the band. However, the computed conductance, for not too small disorder or coupling to the leads (of the same transverse width as the sample),^{46,47} is practically equal to the “intrinsic” conductance $g = E_{Th}/\Delta$ expressed in terms of the spectral properties of a closed sample.

The conductance and density of states (DoS)

$$N(E) = 2 \frac{\rho(E)}{V}, \quad (8)$$

are plotted on Fig. 6. The DoS is obtained from the histogram of the number of eigenstates which fall into equally spaced energy bins along the band. The conductance and DoS of the RH model have a peak at

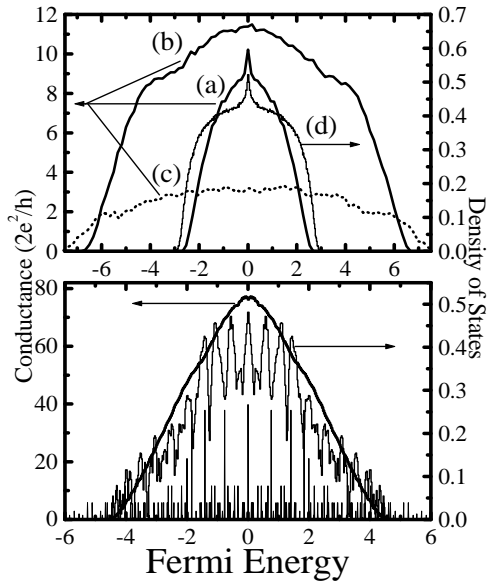


FIG. 6. Conductance and density of states in the RH and DD Anderson models on a simple cubic lattice with $N = 16^3$ sites. Top: RH disorder, (a) and (d), of strength $W_{RH} = 1$ (mobility edge is at $|E_c| \simeq 2.53$); diagonal disorder of strength (b) $W_{DD} = 6$ ($|E_c| \simeq 6.5$), and (c) $W_{DD} = 10$ ($|E_c| \simeq 7.4$). Disorder averaging is performed over $N_{Ens} = 20$ different samples for conductance and $N_{Ens} = 40$ for DoS. Bottom: RH disorder $W_{RH} = 0.25$; sharp lines correspond to the DoS of a clean system on the same lattice (scaled by 1/10 for clarity).

$E = 0$, which becomes a logarithmic singularity in the limit of infinite system size.³⁹ For weak off-diagonal disorder ($W_{RH} = 0.25$), $N(E)$ still resembles the DoS of a clean system, even after ensemble averaging (lower panel of Fig. 6). On the other hand, the conductance is a smooth function of energy since discrete levels of an isolated sample are broadened by the coupling to leads. The same is true for DoS computed from the imaginary part of the Green function for an open system. The mobility edge is absent at low RH disorder ($W_{RH} = 0.25$ and $W_{RH} = 0.375$) for system sizes $L \leq 16a$. This means that localization length ξ is greater than $16a$ (lattice spacings is denoted by a) for all energies inside the band of these systems. For other samples on Fig. 6 the mobility edge appears inside the band. This is clearly shown for $W_{RH} = 1$ case where band edge E_b ($N(E_b) = 0$) differs from E_c . The mobility edge is located at the minimum energy $|E_c|$ for which $g(E_c)$ is still different from zero. The conductance of finite samples is always finite, although exponentially small at $|E_F| > |E_c|$. The approximate values of $|E_c|$ listed on Fig. 6 are such that conductance satisfies: $g(E_F) < 0.1$, for $|E_F| > |E_c|$; typically $g(E_c) \in (0.2, 0.5)$ is obtained, like in the recent detailed studies⁴⁸ of conductance properties at E_c . Thus found E_c is virtually equal to the true mobility edge, defined only in thermodynamic limit (and is usually obtained from some numerical finite-size scaling procedure²). Namely,

the position of mobility edge extracted in this way will not change⁴⁹ when going to larger system sizes if $\xi < L$ for all energies $|E| > |E_c|$.

The distribution $f(t)$ of eigenfunction intensities has been studied analytically for diffusive conductors close to the universal limit (where conductance is large and localization effects are small) in Refs. 16,21 using the supermatrix σ -model,¹¹ or by means of a direct optimal fluctuations method in Ref 50. Numerical studies^{9,51} were conducted in 2D and 3D for all disorder strengths. Here I show how $f(t)$ evolves in 3D disordered samples where a genuine LD transition occurs. The complete eigenproblem of a single particle disordered Hamiltonian is solved numerically, and $f(t)$ is computed as a histogram of intensities for the chosen eigenstates in: metallic phase ($|E| < |E_c|$), insulating phase ($|E| > |E_c|$), and close to the mobility edge $|E_c|$. The two delta functions in Eq. (1) are approximated by a box function $\bar{\delta}(x)$. The width of $\bar{\delta}(E - E_\alpha)$ is small enough at a specific energy that $\rho(E)$ is constant inside that interval. For each sample, 5–10 states are picked by the energy bin, which effectively provides additional averaging over the disorder (according to ergodicity^{12,15} in RMT). The amplitudes of wave functions are sorted in the bins defined by $\bar{\delta}(t - |\Psi_\alpha(\mathbf{r})|^2 V)$ whose width is constant on a logarithmic scale. The function $f(t)$ is computed at all points inside the sample, i.e., $N = 16^3$ in Eq. (1).

The evolution of $f(t)$, when sweeping the band through the “interesting” states, is plotted on Figs. 2, 3 for the RH disordered sample. Since pre-localized states generate slow decay of $f(t)$ at high wave function intensities (where PT distribution is negligible),¹¹ this region is enlarged on Fig. 3. This is obvious from the “pre-localized” example in Fig. 1 where state with large amplitude spikes, highly unlikely in the framework of RMT, was found in a very good metal. The same is trivially true for the localized states which determine extremely long tails of $f_\xi(t)$ (4). Thus, the asymptotic tails of $f(t)$, appreciably deviating from PT distribution, are signaling the onset of localization. It is interesting that states in the band center of RH model, which define the largest zero-temperature conductance [$g(E_F = 0) \approx 10.2$, $\text{Var } g(E_F = 0) \approx 0.63$], are mostly pre-localized. Namely, both the frequency of their appearance and high amplitude splashes resembles the situation at criticality. It might be conjectured that these pre-localized states would generate multifractal scaling of IPR in the band center. This result, together with the DoS and conductance from Fig. 6, shows that phenomena in the band center of 3D conductors with off-diagonal disorder are as intriguing as their much studied counterparts in low-dimensional systems.^{37,38} The origin of these phenomena can be traced back to a special sublattice, or “chiral”,^{36,52} symmetry (leading to an eigenspectrum which for E_n contains $-E_n$ as well, Fig. 5) obeyed by TBH (2) with random hopping (and constant on-site energy). In the cases with $W_{\text{RH}} = 0.25$ or $W_{\text{RH}} = 0.375$ all states are extended. Their $f(t)$ overlaps with the distribution

function for the delocalized states at $E = 1.5$ in the sample characterized by $W_{\text{RH}} = 1$. The distribution function $f_\xi(t)$ in Eq. (4), obtained from the simple parameterization of a localized state, does not fit precisely the numerical result for the states corresponding to $E = 2.75$. An estimate of the localization length, $\xi \simeq 5.5a$, would generate a distribution with a similar tail to that of the analyzed states.

The same statistical analysis is performed for the eigenstates of DD Anderson model—“standard model” in the localization theory.^{2,42,54} Figure 4 plots $f(t)$ at specific energy E_i in samples characterized by different conductance $g(E_F = E_i)$ (controlled by W_{DD}). The conductance $g(E = 0)$ of TBH with $W_{\text{DD}} = 6$ is numerically close to the conductance of RH disordered samples with $W_{\text{RH}} = 1$. Nevertheless, comparison of the corresponding distribution functions reveals model dependent features¹⁶ which are beyond corrections accounted by the eigenmodes of a classical diffusion operator^{32,53} (the spectrum of $\mathcal{D}\nabla^2$, with appropriate boundary conditions, depends on g , shape of the sample and dimensionality). In both models, all computed $f(t)$ intersect PT distribution (from below) around $6 \lesssim t \lesssim 10$, and then develop tails far above PT values. The length of the tails is defined by the largest amplitude exhibited in the pre-localized state, e.g., Fig. 1. For strong DD ($W_{\text{DD}} = 10$) the conductance $g(E_F)$ is smaller than 3.5. In this regime transport becomes “intrinsically diffusive”,⁵⁴ but one can still extract resistivity from the approximate Ohmic scaling of disorder-averaged resistance⁵⁴ (for those fillings where⁵⁵ $g(E_F) > 2$). However, the close proximity to the critical region $g \sim 1$ induces long tails of $f(t)$ at all energies throughout the band—a sign of increased frequency of appearance of highly inhomogeneous states. This provides an insight into the microscopic structure of eigenstates which carry the current in a non-perturbative transport regime^{11,56} (characterized by the lack of semi-classical concepts, like mean free path ℓ , where unwarranted use of the Boltzmann theory would give⁵⁴ $\ell < a$).

In conclusion, the statistics of eigenstates in 3D samples, modeled by the tight-binding Hamiltonian on a simple cubic lattice with $N = 16^3$ sites, have been studied. The disorder is introduced either in the potential energy (diagonal) or in the hopping (off-diagonal) matrix elements. Also calculated are the average Inverse Participation Ratio of eigenfunctions as well the conductance of different samples as a function of energy. This comprehensive set of parameters makes it possible to compare the eigenstates in 3D nanoscale mesoscopic conductors with different types of disorder, but characterized by similar values of conductance. Sample-specific details, which are not parameterized by the conductance alone, are found. This is in spite of the fact that dimensionality, shape of the sample, and conductance (i.e., the eigenvectors and eigenvalues of the classical diffusion operator) are expected to determine the finite-size (non-universal) corrections to the universal (sample-independent) predictions of Random Matrix Theory. The appearance

of states with large amplitude spikes on the top of RMT like background is clearly demonstrated even in good metals. At criticality, such “pre-localized” states are directly related to the extensively studied multifractal scaling of IPR. However, even in the delocalized metallic ($g \gg 1$) phase, where the correlation length⁶ ξ_c expected from the sample conductance $g(\xi_c) = \mathcal{O}(1)$ is microscopic ($L < \xi_c$ would naturally account for the multifractal scaling,⁶ like in 2D), pre-localized state are found in the band center of random hopping disordered systems. They are inhomogeneous enough to generate extremely long (critical like) tails of the distribution of eigenfunction amplitudes.

Inspiring discussions with V. Z. Cerovski are acknowledged. Valuable suggestions and guidance have been provided by P. B. Allen. The important improvements of the initial cond-mat preprint are the result of correspondence with B. Shapiro and I. E. Smolyarenko. This work was supported in part by NSF grant no. DMR 9725037.

‡ Present address: Department of Physics, Georgetown University, Washington, DC 20057-0995.

- ¹ P. W. Anderson, Phys. Rev. **109**, 1492 (1958).
- ² B. Kramer and A. MacKinnon, Rep. Prog. Phys. **56**, 1469 (1993).
- ³ P.A. Lee and T.V. Ramakrishnan, Rev. Mod. Phys. **57**, 287 (1985).
- ⁴ E. Abrahams, P. W. Anderson, D. C. Licciardello, and T. V. Ramakrishnan, Phys. Rev. Lett. **42**, 673 (1979).
- ⁵ *Mesoscopic Quantum Physics*, edited by E. Akkermans, J.-L. Pichard, and J. Zinn-Justin, Les Houches, Session LXI, 1994 (North-Holland, Amsterdam, 1995).
- ⁶ M. Janssen, Phys. Rep. **295**, 1 (1998).
- ⁷ B. L. Altshuler, V. E. Kravtsov, and I. V. Lerner, in *Mesoscopic phenomena in solids*, edited by B. L. Altshuler, P. A. Lee, and R. A. Webb (North-Holland, Amsterdam, 1991).
- ⁸ B. Shapiro, Phil. Mag. B **56**, 1031 (1987).
- ⁹ K. Müller, B. Mehlig, F. Milde, and M. Schreiber, Phys. Rev. Lett. **78**, 215 (1997).
- ¹⁰ V. Uski, B. Mehlig, R. A. Römer, M. Schreiber, cond-mat/0005380.
- ¹¹ K. B. Efetov, *Supersymmetry in Disorder and Chaos* (Cambridge University Press, Cambridge, 1997).
- ¹² C. W. J. Beenakker, Rev. Mod. Phys. **69**, 731 (1997).
- ¹³ *Chaos in Quantum Physics*, edited by M.-J. Jianonni, A. Voros, and J. Zinn-Justin, Les-Houches, Session LII, 1989 (North-Holland, Asterdam, 1991).
- ¹⁴ E. Akkermans and G. Montambaux, Phys. Rev. Lett. **68**, 642 (1992).
- ¹⁵ T. Ghur, A. Müller-Groeling, and H. A. Widenmüller, Phys. Rep. **299**, 189 (1998).
- ¹⁶ For a recent comprehensive review see: A. D. Mirlin, Phys. Rep. **326**, 259 (2000).
- ¹⁷ B. A. Muzykantskii and D. E. Khmelnitskii, Phys. Rev. B **51** 5480 (1995).

- ¹⁸ J. A. Folk *et al.*, Phys. Rev. Lett. **76**, 1699 (1996); A. M. Chang *et al.*, Phys. Rev. Lett. **76**, 1695 (1996).
- ¹⁹ P. Pradhan and S. Sridhar, Phys. Rev. Lett. **85**, 2360 (2000).
- ²⁰ Y. V. Fyodorov and A. D. Mirlin, Phys. Rev. B **51**, 13 403 (1995).
- ²¹ V. I. Fal'ko and K. B. Efetov, Phys. Rev. B **52**, 17 413 (1995).
- ²² The usage of the term “pre-localized” (or anomalously localized) in 3D systems is somewhat ambiguous, e.g., compare Refs. 6,16,21,50.
- ²³ E. J. Heller, Phys. Rev. Lett. **53**, 1515 (1984).
- ²⁴ L. P. Gor'kov, A. I. Larkin, and D. E. Khmel'nitskii, Pis'ma Zh. Eksp. Teor. Fiz. **30**, 248 (1979) [JETP Lett. **30**, 228 (1979)].
- ²⁵ S. Chakravarty and A. Schmid, Phys. Rep. **140**, 195 (1986).
- ²⁶ Note that random Hamiltonians of real disordered solids are tied to the real-space representation (i.e., matrix elements in this representation are spatially dependent, and e.g., TBH (2) is a band diagonal matrix. Therefore, they do not satisfy the statistical assumptions of standard RMT ensembles since all elements of random matrices in RMT are non-zero and spatially independent.²⁷ Nevertheless, the connection to RMT statistics is provided by Efetov's supersymmetric approach.¹¹
- ²⁷ Y. V. Fyodorov, in Ref. 5.
- ²⁸ L. P. Gor'kov and G. M. Eliashberg, Zh. Eksp. Teor. Fiz. **48**, 1407 1965 [Sov. Phys. JETP **21** 1965].
- ²⁹ C. E. Porter and R. G. Thomas, Phys. Rev. **104**, 483 (1956).
- ³⁰ V. I. Fal'ko and K. B. Efetov, Phys. Rev. B **50**, R11 267 (1994).
- ³¹ B. L. Altshuler and B. I. Shklovskii, Zh. Eksp. Teor. Fiz. **91**, 220 (1986) [Sov. Phys. JETP **64**, 127 (1986)]; V. E. Kravtsov and A. D. Mirlin, Pis'ma Zh. Eksp. Theor. Fiz. **60**, 645 (1994) [JETP Lett. **60**, 656 (1994)]; A. V. Andreev and B. L. Altshuler, Phys. Rev. Lett **75**, 902 (1995).
- ³² V. N. Prigodin and B. L. Altshuler, Phys. Rev. Lett. **80**, 1944 (1998).
- ³³ B. I. Shklovskii, B. Shapiro, B. R. Sears, P. Lambrianides and H. B. Shore, Phys. Rev. B **47**, 11 487 (1993).
- ³⁴ F. Wegner, Z. Phys. B **36**, 209 (1980).
- ³⁵ A. D. Mirlin and F. Evers, Phys. Rev. B **62**, 7920 (2000).
- ³⁶ M. Inui, S. A. Trugman, and E. Abrahams, Phys. Rev. B **49**, 3190 (1994), and references therein.
- ³⁷ P. W. Brouwer, C. Mudry, B. D. Simons, and A. Altland, Phys. Rev. Lett. **81**, 862 (1998).
- ³⁸ V. Z. Cerovski, Phys. Rev. B **62**, 12775 (2000).
- ³⁹ F. J. Dyson, Phys. Rev. **92**, 1331 (1953).
- ⁴⁰ P. W. Brouwer, C. Mudry, and A. Furusaki, cond-mat/9904201.
- ⁴¹ P. Cain, R. A. Römer, and M. Schreiber, Ann. Phys. (Leipzig) **8**, 507 (1999).
- ⁴² K. Slevin, T. Ohtsuki, and T. Kawarabayashi, Phys. Rev. Lett. **84** 3915 (2000).
- ⁴³ R. Landauer, Phil. Mag. **21**, 863 (1970); C. Caroli, R. Combescot, P. Nozieres, and D. Saint-James, J. Phys C **4**, 916 (1971); Y. Meir and N. S. Wingreen, Phys. Rev. Lett. **68**, 2512 (1992).

⁴⁴ S. Datta, *Electronic Transport in Mesoscopic Systems* (Cambridge University Press, Cambridge, 1995).

⁴⁵ B. K. Nikolić and P. B. Allen, *J. Phys. Condens. Matter* **12**, 9629 (2000).

⁴⁶ H. A. Weidenmüller, *Physica A* **167**, 28 (1990).

⁴⁷ D. Braun, E. Hofstetter, A. MacKinnon, and G. Montambaux, *Phys. Rev. B* **55**, 7557 (1997).

⁴⁸ P. Markoš, *Phys. Rev. Lett.* **83**, 588 (1999).

⁴⁹ M. J. Calderon, J. A. Vergés, and L. Brey, *Phys. Rev. B* **59**, 4170 (1999).

⁵⁰ I. E. Smolyarenko and B. L. Altshuler, *Phys. Rev. B* **55**, 10 451 (1997).

⁵¹ V. Uski, B. Mehlig, R. A. Römer, M. Schreiber, *Physica B* **284-288**, 1934 (2000).

⁵² A. Altland and B. D. Simons, *J. Phys A* **32**, L353 (1999).

⁵³ A. D. Mirlin and Y. V. Fyodorov, *J. Phys. A* **26**, L551 (1993).

⁵⁴ B. K. Nikolić and P. B. Allen, cond-mat/0005389 (to appear in *Phys. Rev. B Rapid Communications*).

⁵⁵ T. N. Todorov, *Phys. Rev. B* **54**, 5801 (1996).

⁵⁶ B. L. Altshuler and B. D. Simons, in Ref. 5.